PHYSICAL REVIEW D **87,** 081501(R) (2013)

Nonlinear collapse in the semilinear wave equation in AdS space

Steven L. Liebling
Department of Physics, Long Island University, Brookville, New York 11548, USA
(Received 8 January 2013; published 11 April 2013)

Previous studies of the semilinear wave equation in Minkowski space have shown a type of critical behavior in which large initial data collapse to singularity formation due to nonlinearities while small initial data does not. Numerical solutions in spherically symmetric anti–de Sitter space are presented here which suggest that, in contrast, even small initial data collapse eventually. Such behavior appears analogous to the recent result of Bizoń and Rostworowski [Phys. Rev. Lett. **107**, 031102, 2011] that found that even weak, scalar initial data collapse gravitationally to black hole formation via a weakly turbulent instability. Furthermore, the imposition of a reflecting boundary condition in the bulk introduces a cutoff, below which initial data fails to collapse. This threshold appears to arise because of the dispersion introduced by the boundary condition.

DOI: 10.1103/PhysRevD.87.081501 PACS numbers: 04.25.dc

I. INTRODUCTION

Recently, numerical studies of the gravitational collapse of a scalar field in asymptotically anti–de Sitter (AdS) space found that the scalar field collapses to a black hole eventually for *any* initial amplitude for generic initial data [1,2]. This inevitability of black hole formation is understood as thermalization within the corresponding conformal field theory (CFT) on the boundary of AdS according to AdS/CFT correspondence. The nature of the boundary of AdS is such that it can be reached in finite time and therefore the bulk is a bounded domain. As noted in Ref. [1], there is evidence for similar nonlinear behavior in other, nongravitational systems in bounded domains.

It is in the context of such studies that one considers the dynamics of the semilinear wave equation in AdS for a complex scalar field ϕ with a nonlinear potential term ϕ^p where p is an odd integer. Previous studies of this model (for a real scalar field) in Minkowski space have shown that for $p = 7$, the scalar field "collapses" to singularity formation for large initial data and disperses for small initial data [3,4]. In AdS space, one might suspect that even small initial data, which would otherwise disperse in Minkowski space, would instead reflect off the AdS boundary repeatedly and eventually collapse. Indeed, numerical solutions presented here suggest that such behavior is present for the semilinear equation. Furthermore, placing a reflecting boundary at some finite radius places a lower limit on the size of collapsing initial data, similar to that found in the gravitating case [5]. Some speculation about the nature of this change in behavior is given.

II. IMPLEMENTATION

Adopting essentially the same notation and form as in Ref. [5], the metric is assumed to be that of spherically symmetric AdS,

$$ds^2 = \frac{\ell^2}{\cos^2 x}(-dt^2 + dx^2 + \sin^2 x d\Omega_{d-1}^2), \tag{1}$$

where ℓ is the scale size of the AdS spacetime and $d\Omega_{d-1}^2$ is the metric of S^{d-1}. The domain extends from the origin, $x = 0$, to the boundary of AdS, $x = \pi/2$. Introducing the auxiliary quantities $\Phi_i \equiv (\partial/\partial x)(\phi_i)$ and $\Pi_i \equiv (\partial/\partial t)(\phi_i)$, one rescales according to

$$\hat{\phi}_i \equiv \frac{\phi_i}{\cos^{d-1} x}, \tag{2}$$

$$\hat{\Pi}_i \equiv \frac{\partial_t \phi_i}{\cos^{d-1} x} = \frac{\Pi_i}{\cos^{d-1} x}, \tag{3}$$

$$\hat{\Phi}_i \equiv \frac{\partial_x \phi_i}{\cos^{d-2} x} = \frac{\Phi_i}{\cos^{d-2} x}. \tag{4}$$

Here, ϕ_i for $i = 1, 2$ indicates the real and imaginary components of the scalar field. The second-order nonlinear wave equation becomes a system of three first-order equations,

$$\dot{\hat{\phi}}_i = \hat{\Pi}_i, \tag{5}$$

$$\dot{\hat{\Phi}}_i = \frac{1}{\cos^{d-2} x}(\cos^{d-1} x \hat{\Pi}_i)_{,x}, \tag{6}$$

$$\dot{\hat{\Pi}}_i = \frac{1}{\sin^{d-1} x}\left(\frac{\sin^{d-1} x}{\cos x}\hat{\Phi}_i\right)_{,x} + (|\hat{\phi}|\cos^{d-1} x)^{p-1}\hat{\phi}_i. \tag{7}$$

The $U(1)$ symmetry of the complex scalar field results in a conserved charge given by

$$Q = \int_0^{\pi/2} dx \tan^{d-1} x \cos^{2(d-1)} x(\hat{\Pi}_1\hat{\phi}_2 - \hat{\Pi}_2\hat{\phi}_1). \tag{8}$$

The total energy E in the system is computed as

$$E = \int_0^{\pi/2} dx \tan^{d-1} x \cos^{2(d-1)} x \left[\frac{\hat{\Phi}_i^2}{\cos^2 x} + \hat{\Pi}_i^2 + \frac{|\hat{\phi}|^{p+1}}{p+1} \right], \tag{9}$$

where a sum over i is implied. The rescaled scalar quantities are subject to the boundary conditions $\hat{\phi}_i(\pi/2, t) = 0$, $\hat{\Phi}_i(\pi/2, t) = 0$, and $\hat{\Pi}_i(\pi/2, t) = 0$.

The initial data used in this work is generalized from that presented in Ref. [1] and is a subset of that used in Ref. [5],

$$\hat{\phi}_i(x, 0) = \frac{2\epsilon}{\pi} e^{-\frac{4\tan^2 x}{\pi^2 \sigma^2}} \cos^{1-d} x \delta_i^1, \tag{10}$$

$$\hat{\Pi}_i(x, 0) = \omega \hat{\phi}_j(x, 0) \delta_j^1 \delta_i^2, \tag{11}$$

where σ, ϵ, and ω are arbitrary constants. The initial profile for $\hat{\Phi}$ is determined by the spatial derivative of the initial scalar field,

$$\hat{\Phi}_i(x, 0) = (1 - d) \tan^{d-2} x \hat{\phi}_i + \cos^{d-1} x \hat{\phi}_{i,x}. \tag{12}$$

For $\omega \neq 0$, the initial data is charged.

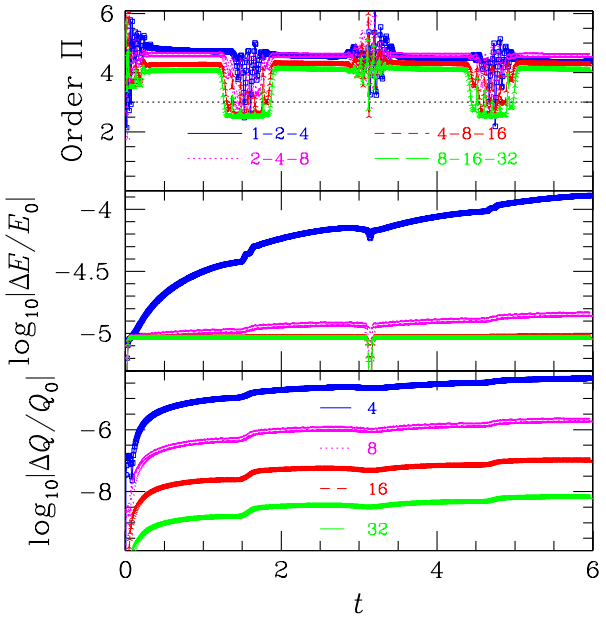

FIG. 1 (color online). Demonstration of convergence through a bounce with $\epsilon = 1$ and $\omega = 5$. Runs with successively doubled resolutions are compared, where the run indicated as "32" has a resolution smaller by a factor of 2^5 than the base resolution run "1." Top: The order of convergence for the field Π_1 as a function of time is shown. The other fields converge similarly. Runs were carried out with multiples as shown of a base resolution. The plot shows that the scheme is generally accurate roughly to fourth order, except when the pulse is at a boundary where it drops to third order. Middle: The fractional change in energy $\log_{10}|E(t) - E(0)|/E(0)$ as a function of time for the four highest-resolution runs. The conservation of energy improves rapidly with resolution and conserves energy to better than about one part in 10^5. Bottom: The fractional change in charge versus time. The conservation similarly improves with resolution.

As discussed in Refs. [3,4], when the amplitude of the scalar field becomes large, the nonlinear potential term dominates and focuses the scalar pulse, leading to singularity formation at some collapse time t_c. Numerically, such collapse is "detected" by stopping the code when $|\phi| \geq 10$, where the value 10 is arbitrary.

These equations are solved using the same infrastructure and methods described in Ref. [1], although no dynamical evolution of metric variables is required as AdS is treated as a fixed background. Tests of the code indicate that it converges to better than third order in the grid spacing and conserves total charge and energy. The convergence order and fractional changes in energy and charge are presented for a typical run in Fig. 1.

III. RESULTS

Typical results are represented in Fig. 2. Charged (blue open circles), uncharged (cyan stars), and charged higher-dimensional (magenta, solid squares) evolutions are shown for a wide range of ϵ. The collapse times get progressively longer (roughly in multiples of the crossing time π). The important point here is that the scalar executes an

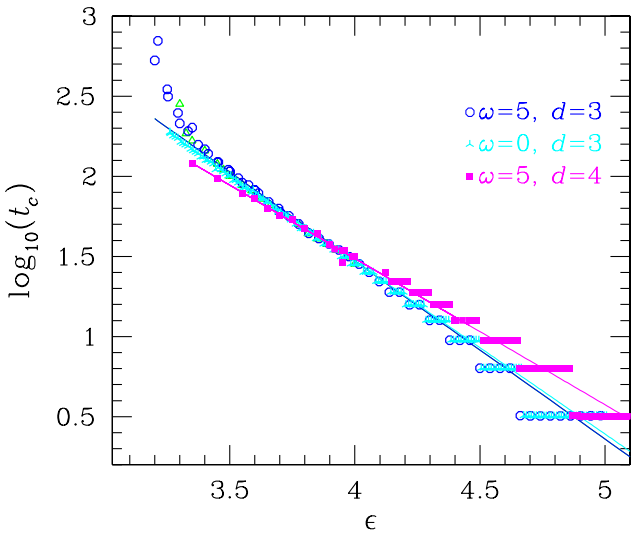

FIG. 2 (color online). Time to collapse as a function of ϵ in the initial data. As ϵ decreases, the initial pulse executes more bounces and the collapse time increases. The jumps in the collapse times shown correspond to the initial pulse executing another bounce and therefore collapse occurs roughly in multiples of $\Delta t = \pi$. Collapse times roughly follow $\log_{10}(t_c) = A\epsilon + B$. Compare to the bottom frame of Fig. 1 of Ref. [2], which shows the time of collapse to black hole for a scalar field. Charged (blue, open circles) initial data follows a trendline with $A = -1.11$ and $B = 5.91$, while uncharged (cyan stars) configurations follow $A = -1.08$ and $B = 5.78$. A charged configuration in $d = 4$ (magenta solid squares) follows a slightly less negative trend with $A = -0.914$ and $B = 5.14$. A few higher-resolution results for $\omega = 5$, $d = 3$ are also shown (open, green triangles), appearing largely consistent with the normal-resolution data.

increasing number of reflections off the boundary with decreasing ϵ and eventually collapses.

As also found in Ref. [5] for the gravitating scalar, the global charge does not appear to have any significant effect. A careful reader might observe, however, that collapse times of the charged family in $d = 3$ rises quite sharply at small ϵ. For such long runtimes, higher resolution is generally called for, despite the use of adaptive mesh refinement because of the accumulation of error, and higher-resolution results are shown in green, open triangles. The two resolutions mostly agree with each other, and so perhaps this rapid rise in collapse times is evidence of some physical effect of either the charge or other difference in the initial data. An example of one such property of initial data resulting in the rapid rise in collapse times can be found in Ref. [6], but further calculations are needed for this case.

The collapse times for a different family of initial data are shown in Fig. 3. This family is characterized by $\sigma = 1/8$, twice the value characterizing the data shown in Fig. 2. These data similarly suggest scalar collapse is inevitable for any initial amplitude.

Reference [5] studied gravitational collapse on a restricted computational domain by imposing reflecting boundary conditions at some largest value $x_{\max}$ of the coordinate x. In such a space, the scalar pulse does not "see" the full AdS background but nevertheless still evolves within a bounded domain. That the evolutions showed collapse after a number of reflections supported the view that the cause behind the inevitable collapse was that the domain was bounded, not that the space was AdS in particular. The boundedness of the domain allowed for

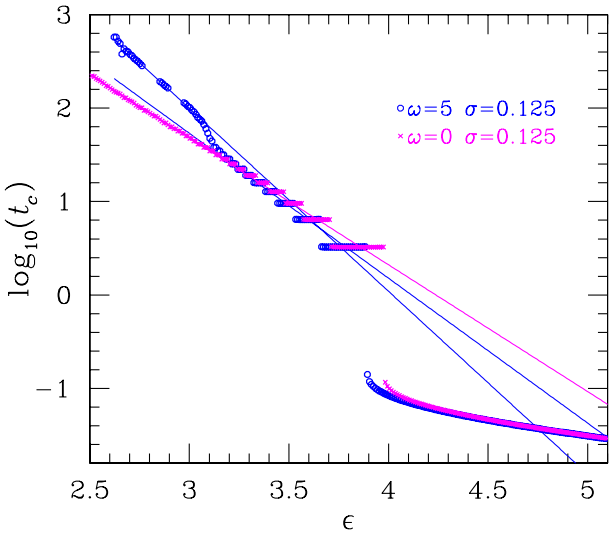

FIG. 3 (color online). Collapse times for families characterized by $\sigma = 0.125$ (in contrast to families with $\sigma = 0.0625$ shown in Fig. 2). Initial data with rotation (blue circles) displays a transition from $A = -1.55$ and $B = 6.38$ to $A = -1.96$ and $B = 7.87$. Initial data without rotation (magenta crosses) follows the trendline described by $A = -1.36$ and $B = 5.75$.

the nonlinearity of gravity to act continuously. However, Ref. [5] also reported that, although collapse did occur after a number of reflections, for a small enough initial amplitude collapse did *not* occur, even after many reflections.

In light of this interesting effect, evolutions of the nonlinear wave equation here are conducted within a restricted domain with the identical, reflecting boundary condition of Ref. [5]. In particular, the scalar field is fixed via enforcement of a Dirichlet condition $\phi_i(x_{\max}, t) = 0$ and $\Pi_i(x_{\max}, t) = 0$. Studies with domains extending only to $x_{\max} = 0.95$, 0.90, 0.85, and $\pi/4 \approx 0.785$ are shown in the top frame of Fig. 4, along with those within the full AdS spacetime ($x_{\max} = \pi/2$) for comparison.

These restricted domain runs behave in stark contrast with the full-domain results. Evolutions which collapse essentially immediately (before any reflection off the boundary) nearly coincide as would be expected. After one reflection, one would expect some range of ϵ values that would result in collapse, and therefore these restricted domains collapse faster than the full-domain evolutions simply because the geometric "concentration" at the origin happens earlier. However, as one considers even smaller ϵ values, one sees that the collapse time grows apparently asymptotically to infinity. In other words, the evolutions suggest the existence of some threshold value of $\epsilon_{\min}$ below which finite-domain evolutions no longer collapse.

As ϵ is decreased in increasingly finer steps near the threshold, more bounces are observed before collapse, as indicated in the top frame of Fig. 4. It is not clear yet what happens in the limit that ϵ approaches some critical $\epsilon_{\min}$, and in particular whether the number of bounces continues to increase.

In the examples shown in the top frame of Fig. 4, this minimum value increases apparently linearly with increasing $x_{\max}$. However, the results of a brief study of $\epsilon_{\min}$ as a function of $x_{\max}$ is shown in the bottom frame and reveals very nontrivial behavior. These values were obtained by a bisection search on ϵ for a given value of $x_{\max}$. Beginning with a bounding bracket $[\epsilon_{\text{low}}, \epsilon_{\text{high}}]$, the evolution of the average $\epsilon_{\text{avg}} = (1/2)[\epsilon_{\text{low}} + \epsilon_{\text{high}}]$ was computed up to a maximum time $t_{\max} = 30$. A new bracket is found such that if collapse occurred then one resets $\epsilon_{\text{high}} = \epsilon_{\text{avg}}$, and otherwise one sets $\epsilon_{\text{low}} = \epsilon_{\text{avg}}$. Most of the computing time is spent on evolutions which do not collapse and therefore limiting $t_{\max}$ greatly speeds up the calculation at the expense of some accuracy. The search is carried out until the fractional difference in the bounds is one ten-thousandth.

It is interesting to note that because the full domain is expected to collapse for any value of ϵ, its respective $\epsilon_{\min}$ is zero. In addition, the results shown in the top frame of Fig. 4 indicate an increasing $\epsilon_{\min}$ with increasing $x_{\max}$. However, as shown in the bottom frame, at large values of $x_{\max}$ this behavior reverses, giving one hope that the limit

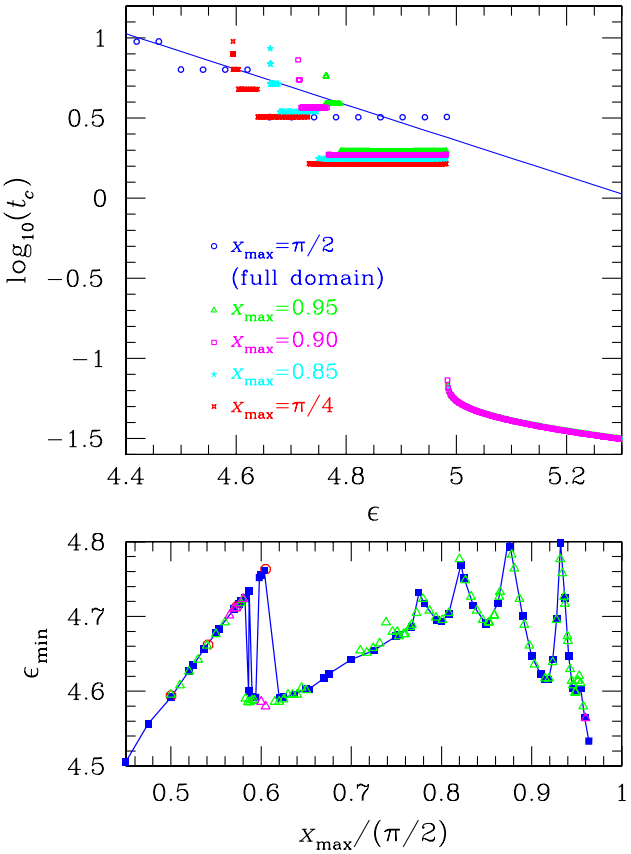

FIG. 4 (color online). Collapse within restricted domains of AdS. Top: Collapse times for various domains extending to x_{max}. The same results for the $\omega = 5$, $d = 3$ evolutions in the full domain from Fig. 2 are shown to facilitate comparison and contrast between full-domain and finite-domain results. Note that as the outer boundary is moved inwards, the minimum value of ϵ that produces collapse decreases. For sufficiently small ϵ, no collapse is detected and therefore collapse times for these runs extend mostly vertically. The collapsing solutions closest to the threshold have values of ϵ within a few parts in a million of the ϵ values of solutions which do not collapse. Bottom: An explicit calculation of the minimum ϵ_{min} for which collapse is detected as a function of x_{max}. To get a sense of how converged these values (blue, solid squares) are, higher-resolution computations (open, green triangles) and higher-resolution computations to later times ($t_{max} = 50$) are also shown. Finally, the ϵ_{min} values (open, red circles) from the data shown in the top frame are also displayed. The apparent linearity of the top frame belies the various features in the full "spectrum."

$x_{max} \to \pi/2$ is smooth. Higher-resolution data and data with a larger value of t_{max} are also shown and appear to support the validity of these surprisingly intricate data. Further calculations are needed especially in the apparently oscillatory region around $x_{max} \approx 0.6$. As noted below, it would also be interesting to compare this behavior with results using a Neumann boundary condition instead.

That small-ϵ, restricted-domain evolutions fail to collapse argues against the idea that the important effect of AdS is its introduction of reflections. Instead, perhaps some other property of AdS accounts for the inevitable collapse and by restricting the domain, this property is affected. That is not the argument presented here. Instead, there appears to be another effect introduced by the restriction of the domain, an effect not seen in the full-domain case.

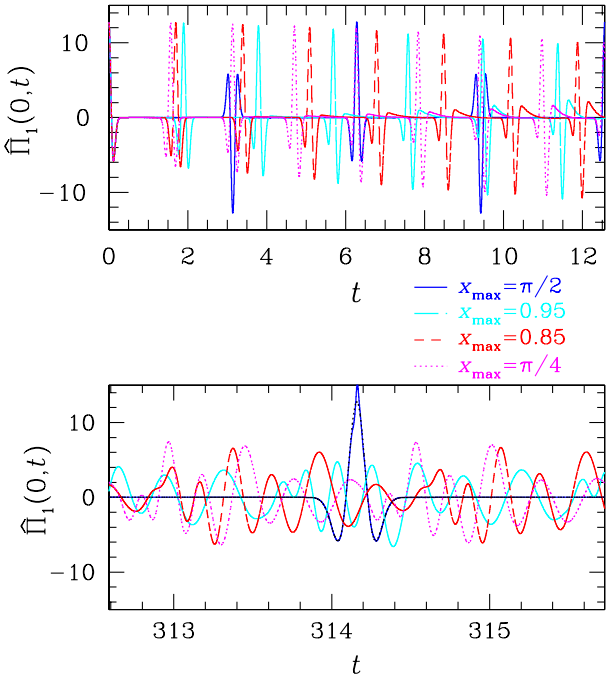

FIG. 5 (color online). Demonstration of dispersion with restricted domain evolutions of the "linear" wave equation. Shown is the behavior of $\hat{\Pi}_1$ at the origin versus time for evolutions in which the nonlinear term ϕ^7 has been removed. The full domain result (solid blue) is shown for reference, which maintains its shape (except for an inversion of sign) with each reflection. The restricted domain evolutions show no inversion but do change shape. The bottom frame shows the late-time behavior where the dispersion of the restricted domain evolutions is quite apparent. Also shown (dotted black) is the full domain pulse from $t \approx \pi$, shifted in time and inverted in sign. That it nearly overlays the late-time, full-domain result indicates a lack of dispersion when evolving in the full AdS space.

Consider the wave equation with no nonlinear term, that is, Eq. (7) without the ϕ^{p-1} term [7]. In spherically symmetric Minkowski space, the solutions take the simple form $r\phi(r, t) = f(r \pm t)$, where r is the radial coordinate and $f()$ is some function. There is no dispersion of $f()$, although $\phi(r, t)$ decreases in amplitude with increasing r. In AdS, however, things are not so simple and one expects that the metric terms will cause dispersion. In Fig. 5, the behavior of $\hat{\Pi}_1(0, t)$ at the origin is shown at various times. In the full domain, the pulse "reflects" off the AdS boundary without inversion and flips when it implodes through the origin. Besides the inversion, the behavior of the pulse remains the same, even at late times. The periodicity results from the fact that the modes of the scalar field in AdS have integer values, and hence a generic initial

configuration will repeat with a period (at most) of $\Delta t = 2\pi$ [8]. In the restricted domains, the pulse inverts at both the outer boundary [9] and the origin, and it disperses. Because the restricted domain does not allow for integer eigenvalues, it is not periodic.

The results suggest that this dispersion competes with the nonlinearity (be it gravitational or simply some scalar potential term). In this way, restricted domain evolutions of small initial data are dominated by the dispersion, whereas strong initial data are instead dominated by the nonlinearity. In the special case where the full domain is allowed, no dispersion occurs, and any initial data will eventually collapse.

IV. CONCLUSIONS

These studies provide an example of a nongravitational, hyperbolic system which results in the sharpening, and eventual collapse, of an initial pulse. This result appears analogous to the gravitational collapse of a scalar field in AdS.

Evolutions within a restricted domain with reflecting boundary conditions also behave similarly to the gravitating scalar [5]. In particular, such evolutions collapse for only a limited range of decreasing amplitude and stop collapsing below some threshold initial size. The imposition of a reflecting boundary condition introduces dispersion where it would otherwise not appear, and this dispersion appears to compete with the weak turbulence [1] that transfers energy to higher frequencies. As one considers smaller initial data, one observes a transition from the dominance of weak turbulence to dispersion.

It should be noted that not all scalar configurations in the gravitating case are unstable [6,10], and it would be interesting to study the $p = 5$ case of the semilinear equation because, at least in Minkowski space, it possesses a static solution [3,4,11].

ACKNOWLEDGMENTS

Thanks go to Alex Buchel, Carsten Gundlach, Luis Lehner, Oscar Reula, and Nikodem Szpak for helpful discussions. This work was supported by the NSF via Grant No. PHY-0969827. Computations were performed thanks to allocations at the Extreme Science and Engineering Discovery Environment (XSEDE), which is supported by National Science Foundation Grant No. OCI-1053575.

[1] P. Bizoń and A. Rostworowski, Phys. Rev. Lett. **107**, 031102 (2011).
[2] J. Jalmuzna, A. Rostworowski, and P. Bizoń, Phys. Rev. D **84**, 085021 (2011).
[3] S. L. Liebling, Phys. Rev. D **71**, 044019 (2005).
[4] P. Bizoń, T. Chmaj, and Z. Tabor, Nonlinearity **17**, 2187 (2004).
[5] A. Buchel, L. Lehner, and S. L. Liebling, Phys. Rev. D **86**, 123011 (2012).
[6] A. Buchel, S. L. Liebling, and L. Lehner (to be published).
[7] Qualitatively identical results are obtained in the appropriately weak-field regime of the full, nonlinear equation.
[8] Thanks to Carsten Gundlach for pointing this out.
[9] One could instead impose a free Neumann boundary condition at some $x_{\max}$ that would not invert the pulse at the outer boundary and thus be more similar to the AdS boundary. However, initial attempts at such a condition proved (numerically) unstable.
[10] O. J. Dias, G. T. Horowitz, D. Marolf, and J. E. Santos, Classical Quantum Gravity **29**, 235019 (2012).
[11] N. Szpak, Theor. Math. Phys. **127**, 817 (2001).